

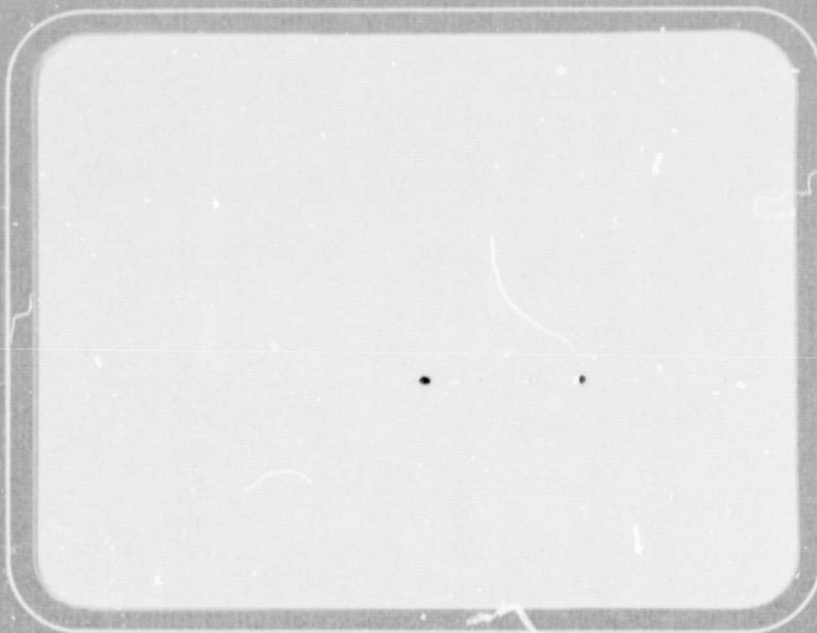
N O T I C E

THIS DOCUMENT HAS BEEN REPRODUCED FROM
MICROFICHE. ALTHOUGH IT IS RECOGNIZED THAT
CERTAIN PORTIONS ARE ILLEGIBLE, IT IS BEING RELEASED
IN THE INTEREST OF MAKING AVAILABLE AS MUCH
INFORMATION AS POSSIBLE



Battelle
Columbus Laboratories

Report



(NASA-CR-161367) EVALUATION OF WORN SSME
LOW PRESSURE LIQUID OXYGEN TURBOPUMP BEARING
Final Report (Battelle Columbus Labs.,
Ohio.) 29 p HC A03/MF A01

CSCL 131

N80-15412

G3/37 Unclass
46593



FINAL REPORT

on

EVALUATION OF WORN SSME LOW PRESSURE
LIQUID OXYGEN TURBOPUMP BEARING

Contract No. NAS8-33576

Task No. 101

to

NATIONAL AERONAUTICS AND SPACE ADMINISTRATION
GEORGE C. MARSHALL SPACE FLIGHT CENTER

by

K. F. Dufrane and J. W. Kannel

December 14, 1979

BATTELLE
COLUMBUS LABORATORIES
505 KING AVENUE
COLUMBUS, OHIO 43201

TABLE OF CONTENTS

	<u>Page</u>
INTRODUCTION.	1
SUMMARY AND RECOMMENDATIONS	2
COMPONENT INSPECTION.	3
Races	3
Balls	10
Cage.	10
LOAD AND STRESS ANALYSIS.	14
Approach for Bearing Calculations	14
Results of Calculations	16
DISCUSSION.	22
Fatigue Considerations.	22
Lubrication Effects	24
Measuring Units	25

LIST OF FIGURES

Figure 1. Talysurf Profile showing Burr at Edge of Race Curvature on Inner Race.	4
Figure 2. Scanning Electron Micrographs of Wear Tracks on Inner Race	6
Figure 3. Scanning Electron Micrographs of Wear Tracks on Outer Race	7
Figure 4. Talyrond Cross-race Curvature Profiles	8
Figure 5. Metallographic Sections of Bearing Races	9
Figure 6. Talyrond Roundness Profiles on Two Balls	11

TABLE OF CONTENTS
(Continued)

LIST OF FIGURES
(Continued)

	<u>Page</u>
Figure 7. Typical Microstructure of Ball.	12
Figure 8. Talysurf Profile of Wear in Cage Ball Pocket.	13
Figure 9. Summary of Race Evaluations	15
Figure 10. Effect of Diametral Clearance Increase on Bearing Contact Angle	18
Figure 11. Effect of Diametral Clearance Increase on Hertz Half Width.	19
Figure 12. Effect of Diametral Clearance Increase on Contact Pressure.	20
Figure 13. Effect of .4 mm (.016 inch) Diametral Clearance Loss and 6000 Pounds Axial Load on Bearing Ball-Race, Contact Dimensions.	21

LIST OF TABLES

Table 1. Parameters Used in Bearing Analysis	17
--	----

EVALUATION OF WORN SSME LOW PRESSURE LIQUID OXYGEN TURBOPUMP BEARING

by

K. F. Dufrane and J. W. Kannel

INTRODUCTION

The bearing analyzed in this study was the larger of two ball bearings used to support the rotor of the low pressure liquid oxygen turbopump in each of the Shuttle main engines. The bearing is an angular contact design with a 85 mm bore, a split inner race, and a glass fiber-reinforced PTFE cage for providing lubrication to the balls and races by a transfer-film mechanism. The bearing serial number was S/N-8383534. The turbopump in which it was used operated for 5000 seconds at 5000 rpm prior to removing the bearing for inspection. In this time period, the axial clearance increased from 0.51 mm (0.020 inch) to 0.89 mm (0.035 inch). Although the bearing reportedly showed no other evidence of distress, an analysis was desired to identify the cause of the excessive internal wear.

Battelle's specific objectives in this study were:

- (1) Perform a microscopic and metallurgical examination of the bearing components,
- (2) Calculate the actual operating loads, their direction, and length of time at each load based on the size and location of the race contact paths,
- (3) Estimate the B_1 life of the bearing, recommend any further efforts required, and specify any design, material, or lubrication changes that would improve the bearing durability.

SUMMARY AND RECOMMENDATIONS

The metallographical and dimensional analyses have indicated that severe wear of the bearing occurred. In its final condition, the bearing wore to the extent that the ball "over-hung" the inner race and a burr was formed outboard of the edge of this race. Based on the analytical studies, it appears that the operating bearing axial load was on the order of 27 KN (6000 pounds). Under this loading, the balls and races wore to the extent that the effective diametral clearance of the bearing increased by .4 mm (.016 inch).

The observed level of wear and concomitant change in bearing contact angle represent very serious problems for the pump bearings. This wear is a result of the severe contact pressures to which the bearing is subjected in concert with the poor lubrication at the ball-race contact. Short term fixes for these problems might be to increase the size of the inner race to allow for a contact angle shift. It would also be desirable to improve the lubrication system to reduce bearing wear. Unfortunately, there are no easy solutions for better lubrication.

The bearing is probably lubricated by a transfer mechanism from the cage to the race. Based on the observed cage wear, a sufficient quantity of this cage material should have been available at the ball-race contact. Despite this plethora of transfer material, however, gross wear occurred because of the magnitude of the bearing pressures (2.3 GPa - (320,000 psi)). Good lubrication can be achieved by transfer film lubrication only if the contact pressures are consistently less than 2 GPa (280,000 psi). It is possible that a bearing pre-treatment (such as with a per-fluorinated ether) could be used to retard wear. However, critical experiments are needed to develop this approach.

The general problem with the bearing as with all bearings in the Shuttle engine is that the contact stresses are too high and the lubrication virtually non-existent in comparison with accepted engineering practices. If the engines are to be successful, serious consideration should be given to modifying component designs to reduce bearing stresses and to enhance lubrication. Such modification would require bearing designs which deviate

considerably from current configuration and would require some change in bearing mounting systems to allow for heavier-duty bearings to be installed. Such modification must be accompanied by basic studies involving cryogenic transfer-film lubrication and pre-treatment evaluations to guide the design changes.

It is our recommendation that NASA consider implementing a bearing design modification program as soon as possible before bearing failures become Shuttle failures. Such a program would be multi-disciplinary and would encompass several organizations including Battelle, NASA, and Rocketdyne.

COMPONENT INSPECTION

Races

Examination of the races revealed two distinct ball-contact paths on both the outer and one-half of the inner race. The paths were uniform in width and in location, which indicates that the loads were primarily axial and well aligned with the race centerlines. Apparently, any synchronous radial loads (such as from rotor unbalance) were small in comparison with the axial loads.

On the outer race, the highest-contact-angle track extended 2.97 mm (0.117 inch) from the edge of the race chamfer. Of this width, the 0.56 mm (0.022 inch) nearest the chamfer was very mildly worn and had some original finishing scratches still intact. The second track was located adjacent to the first and measured 4.32 mm (0.170 inch) wide, with 0.89 mm (0.035 inch) of mild wear at the edge furthest from the chamfer. The two tracks were distinguishable both by the nature of the wear and by a narrow polished band approximately 0.38 mm (0.015 inch) between them.

The highest-angle wear track on the inner race extended to the edge of the largest inner-race diameter. The original chamfer was not present, and a burr was rolled-up at the corner. The height of the burr was measured to be approximately 0.043 mm (0.0017 inch) from the Talysurf trace shown in Figure 1. The highest-angle track measured 2.11 mm (0.083 inch) in width, while the second track extended from the first track an additional

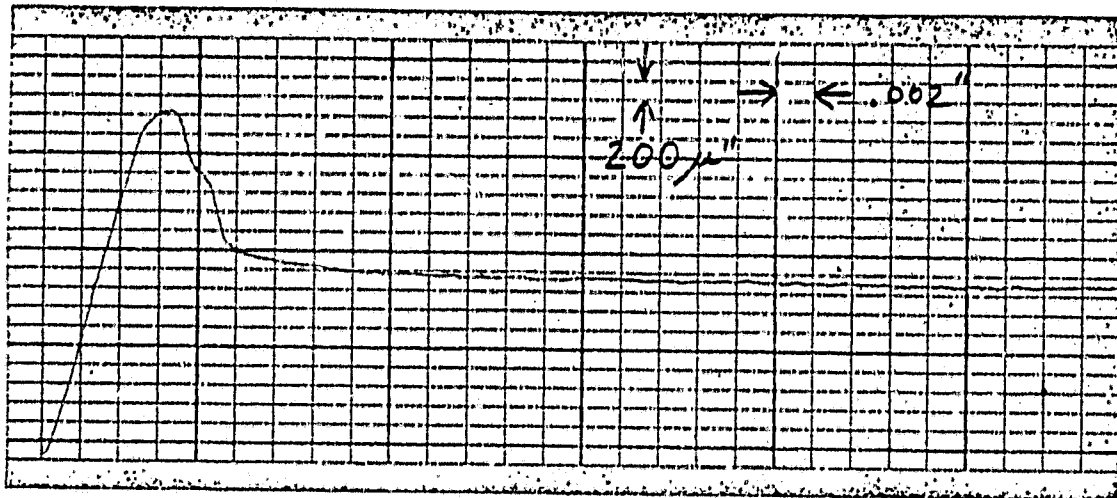


FIGURE 1. TALYSURF PROFILE SHOWING BURR AT EDGE
OF RACE CURVATURE ON INNER RACE

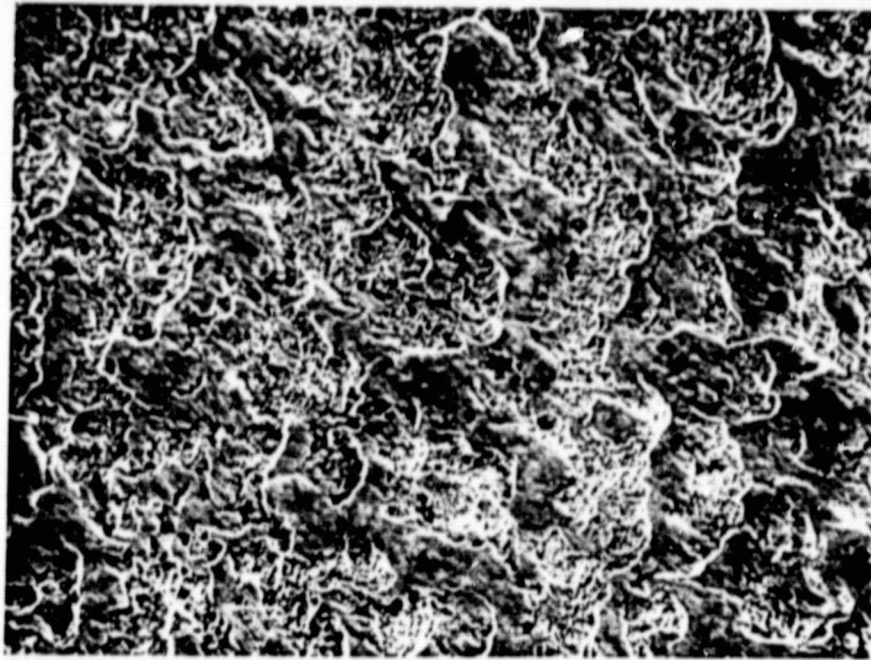
REPRODUCIBILITY OF THE
ORIGINAL PAGE IS POOR

5.08 mm (0.200 inch). A narrow polished area approximately 0.30 mm (0.012 inch) was located at the junction of the two tracks.

Examination of the worn races in the SEM showed the wear to be fairly uniform across the widths of the individual ball-contact paths. The wear patterns consisted of numerous pitted areas separated by raised featureless areas which apparently had been in contact with the balls. Typical areas are shown in Figures 2 and 3. The wear was most severe on the inner races tracks, while the high-angle track on the outer race was least severe. Neither race contained any major pits, gouges, or dents, rather they showed the results of a mild and gradual wear process.

A Talyrond roundness measuring instrument was used to attain cross-race curvature measurements of the races. Gage blocks were set for a reference to measure the diameter of the circle best fitting the race curvature. The two halves of the inner race were clamped together with an 0.20 mm (0.008 inch) shim between them, which the manufacturing drawing specifies to be present during grinding of the curvature. The results of the traces are shown in Figure 4. The measured radii fell within specification for both races. With the unworn band present near the edge of the outer race to serve as a reference, Figure 4(a), an accurate profile was produced on this race. The maximum wear depth was approximately 0.030 mm (0.0012 inch). Since the wear on the inner race extended to the edge of the curvature and since the unworn portion on that half of the race was narrow, no good reference existed for an accurate determination of the wear depth. However, with the assumptions of a uniform original curvature formed in accordance with the drawing regarding the presence of the 0.20 mm (0.008 inch) shim, the maximum wear depth measured in Figure 4(b) is approximately 0.10 mm (0.004 inch).

Metallographic sections prepared of the races showed the near-surface material of the inner race to be plastically deformed to form the burr, Figure 5(a). Thin films of material, measuring approximately 0.0025 mm (0.0001 inch) thick were present in areas on the ball-contact surfaces of both races, as seen in Figures 5(a) and (b). These films are probably PTFE transferred from the cage. No subsurface cracking, extensive deformation or steel transfer was present, which helps to confirm a near-surface wear



300X

24969

a. High contact-angle track



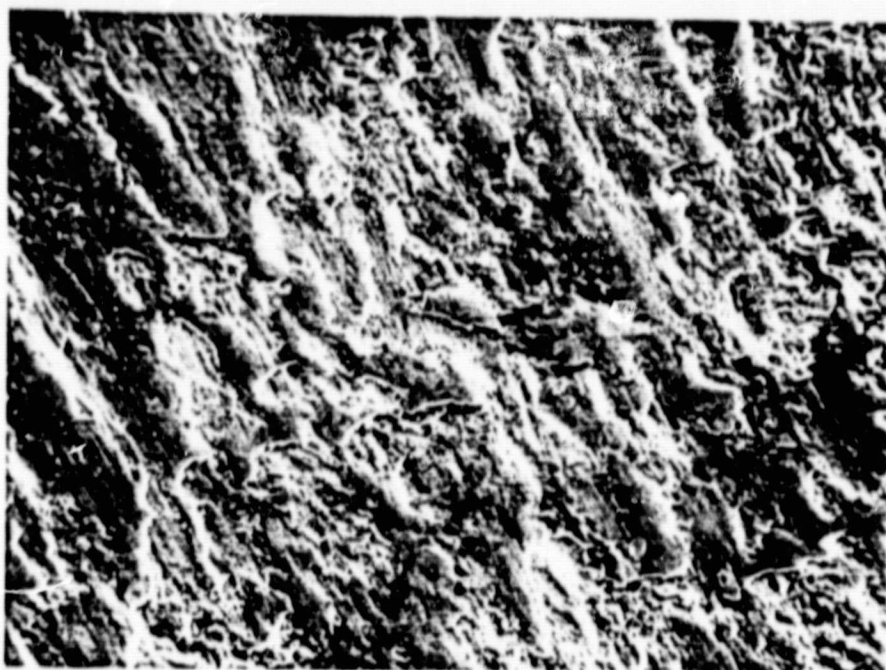
300X

24970

b. Low contact-angle track

FIGURE 2. SCANNING ELECTRON MICROGRAPHS OF WEAR TRACKS ON INNER RACE

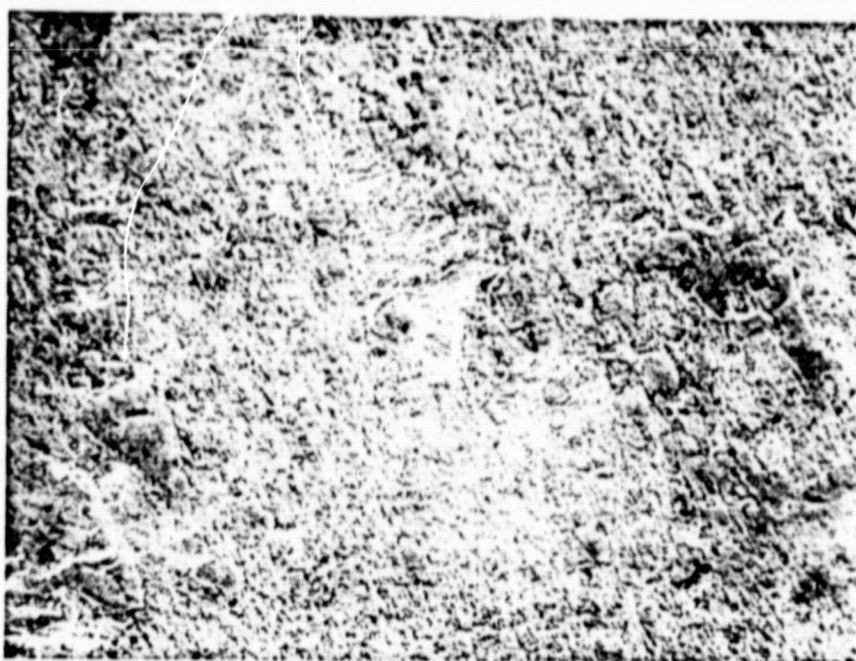
REPRODUCIBILITY OF THE
ORIGINAL PAGE IS POOR



300X

a. High contact-angle track

24972



300X

b. Low contact-angle track

24971

FIGURE 3. SCANNING ELECTRON MICROGRAPHS OF WEAR
TRACKS ON OUTER RACE

REPRODUCIBILITY OF THE
ORIGINAL PAGE IS POOR

REPRODUCED FROM
ORIGINAL PAGE 15 OF 100

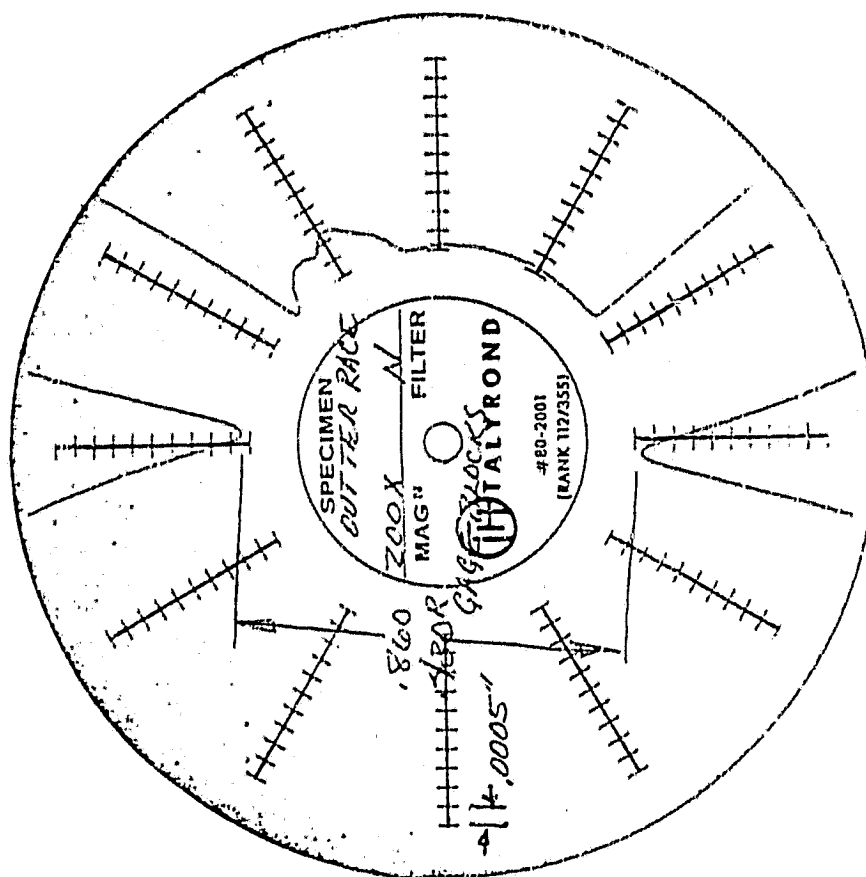
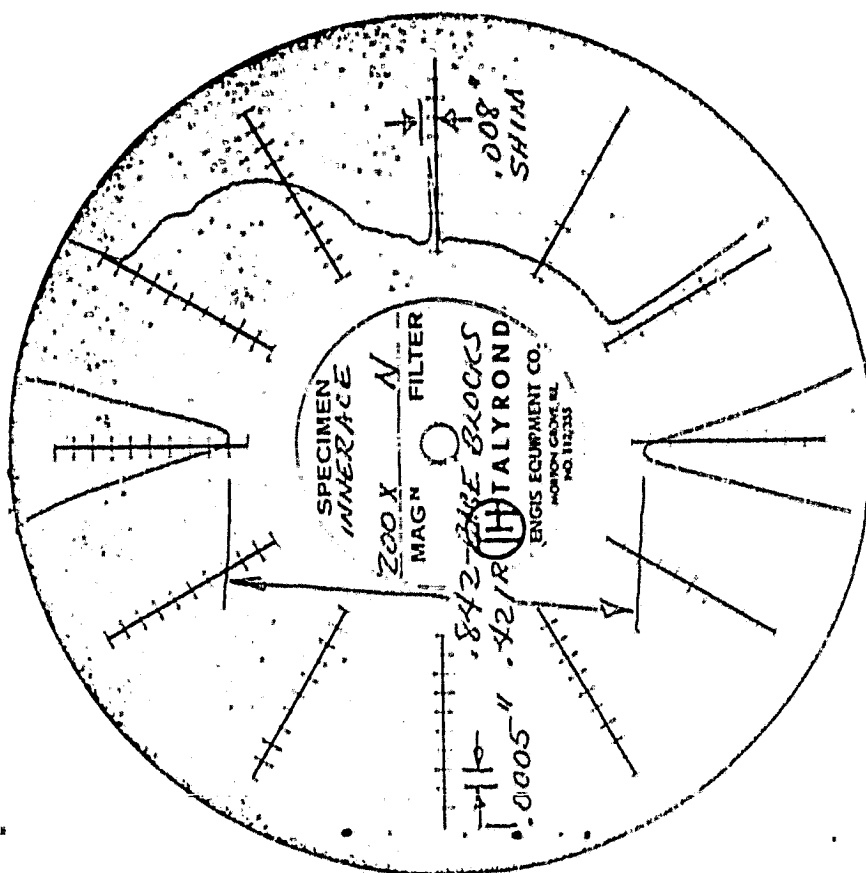
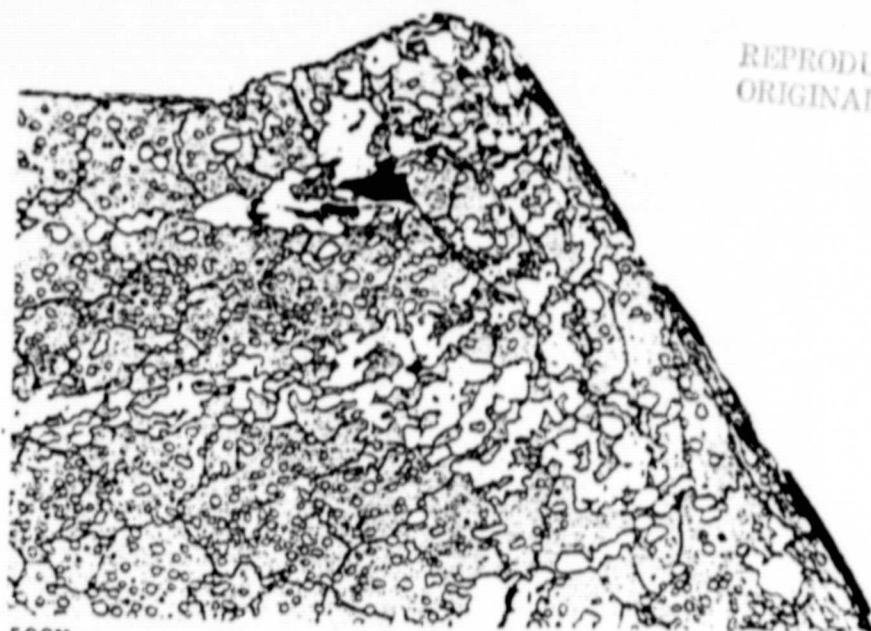


FIGURE 4. TALYSTOND CROSS-FACE CURVATURE PROFILES

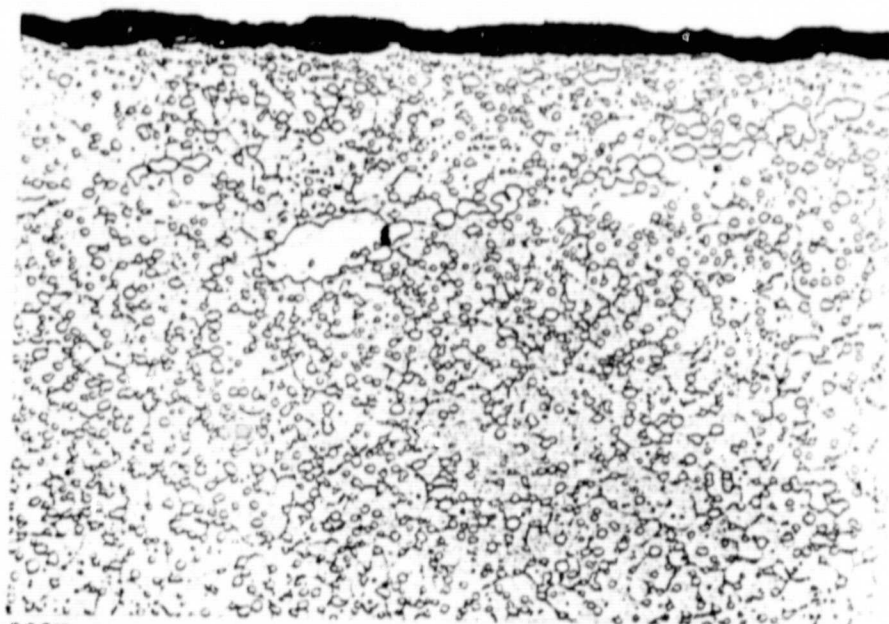
REPRODUCIBILITY OF THE
ORIGINAL PAGE IS POOR



500X

9J425

a. Inner race, showing burr at edge
of race curvature



500X

9J426

b. Outer race

FIGURE 5. METALLOGRAPHIC SECTIONS OF BEARING RACES

process. The microstructure was typical of that expected for 440C bearing steel, and the measured hardness of 59 R_c on the outer race and 58 R_c on the two halves of the inner race were within the expected tolerance.

Balls

The entire set of balls was worn fairly uniformly by approximately 0.076 mm (0.003 inch) on the diameter. There was no indication of heavy banding or pitting, and all balls had a metallic luster. Typical Talysurf traces on two balls are shown in Figure 6. The maximum deviation from roundness was approximately 0.0140 mm (0.00055 inch), which far exceeds the 0.00025 mm (0.000010 inch) of the original AFBMA Grade 10 standard. Therefore, although the balls were fairly uniform on an overall scale, their deviation from roundness is significant.

The typical near-surface microstructure of a ball is shown in Figure 7. No cracking or other sub-surface damage was present that would indicate a wear mechanism other than a mild near-surface material removal process. Similar to the races, patches of film (probably PTFE from the cage) could be seen on the ball cross-section. The hardness of the balls was measured to be 60 R_c .

Cage

The pockets of the cage showed significant wear, as shown by the Talysurf trace in Figure 8. This trace, taken across the pocket from the OD to the ID of the cage in the plane of the ball component, showed a maximum wear depth of approximately 0.17 mm (0.0065 inch). The wear was similar on both the leading and trailing sides of the pockets and was uniform in all of the pockets. There was no significant wear on the outer-race-guiding surfaces or in the pockets in the axial direction of the bearing.

REPRODUCIBILITY OF TI
ORIGINAL PAGE IS POOR

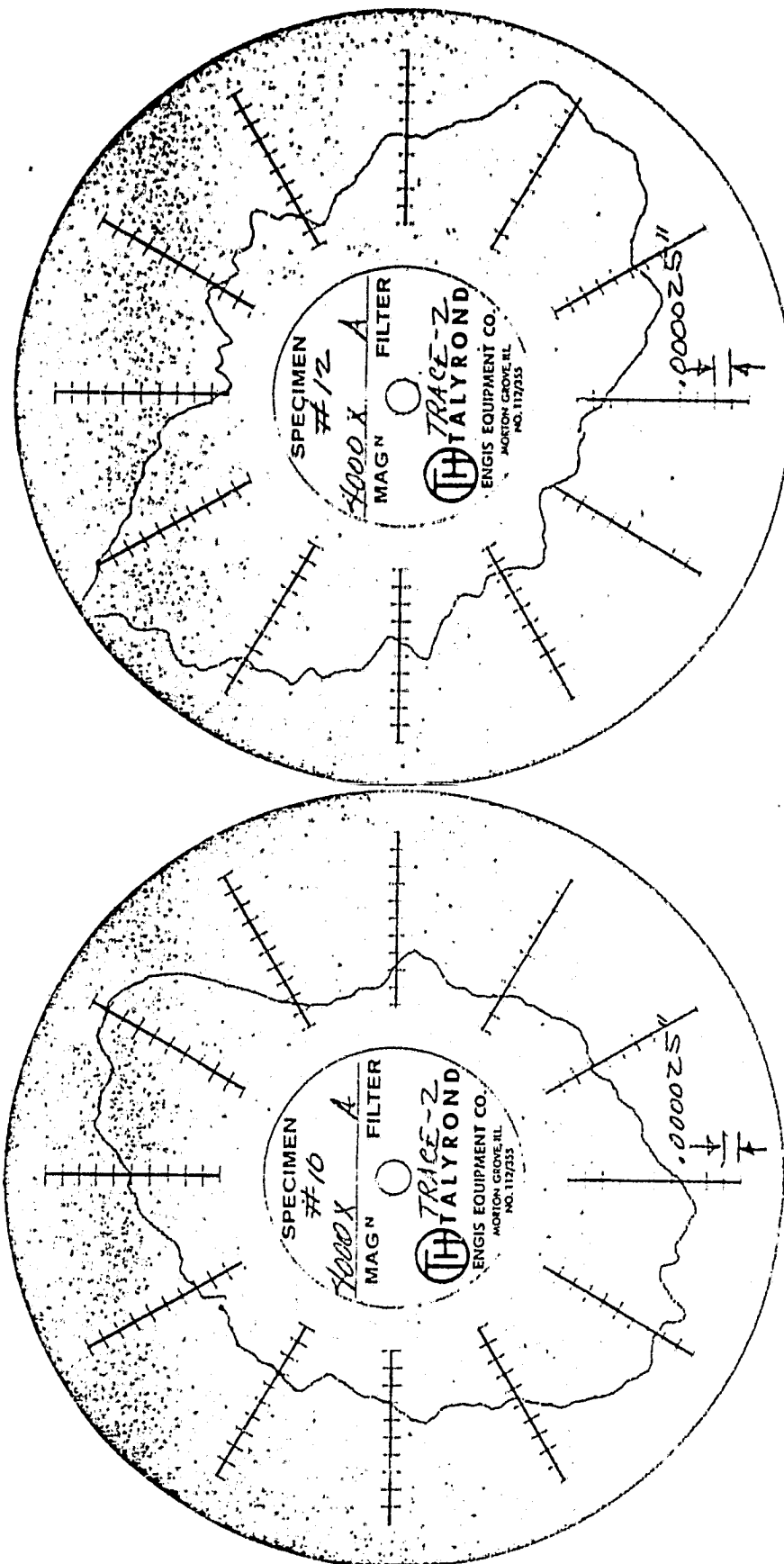


FIGURE 6. TALLYROND ROUNDNESS PROFILES ON TWO BALLS

REPRODUCIBILITY OF THE
ORIGINAL PAGE IS POOR

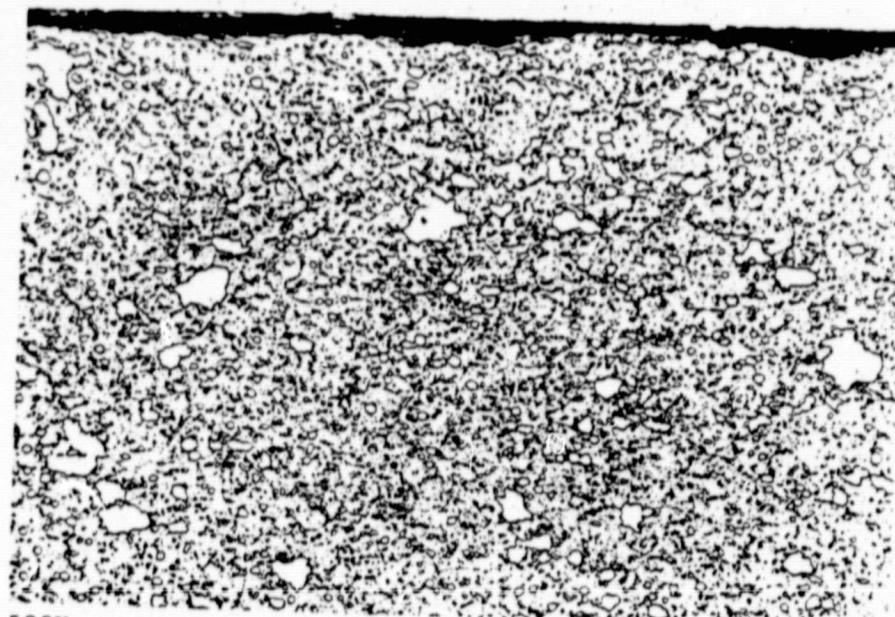


FIGURE 7. TYPICAL MICROSTRUCTURE OF BALL

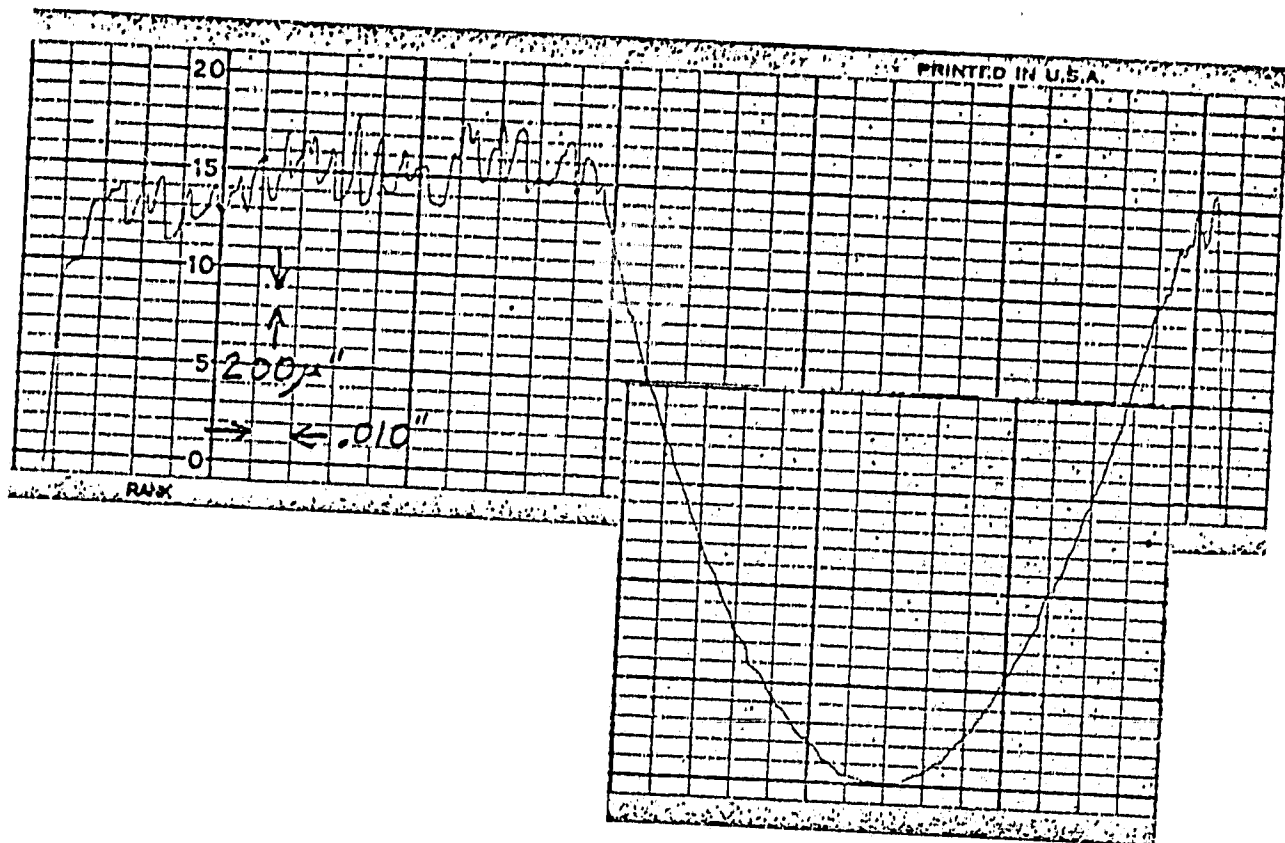


FIGURE 8. TALYSURF PROFILE OF WEAR
IN CAGE BALL POCKET

LOAD AND STRESS ANALYSIS

The bearing inspections have revealed that ball-race contact occurred over a wide portion of both the inner and outer races (Figure 9) and that severe wear occurred on the ball. In addition, it was apparent that the last track of the ball was beyond the edge of the inner race, which resulted in a severe material flow over the edge of the race. These observations strongly suggest that the bearing was in a terminal condition and that continued running would have resulted in a serious failure. The purpose of the analysis is an attempt to understand the progression of the wear mechanism in order to guide corrective action.

Approach for Bearing Calculations

The method for bearing-load computation at Battelle involves the use of a computer program series under the general name, BASDAP. BASDAP programs can be used for static or dynamic analyses of bearings for a wide range of applications. BASDAP programs have been used in static or quasi-dynamic analyses to determine ball-race stresses and ball steady-state motions as well as analyses of dynamic behavior of the cage to determine cage stability and ball-cage loadings. The BASDAP program treats each bearing, in a set, independently.

For the project discussed herein, only a quasi-dynamic version of the BASDAP computer code was utilized. This code involves calculation of ball-race forces (inner and outer), contact pressures, contact dimensions, and contact angles as a function of:

- (1) axial load
- (2) radial load
- (3) centrifugal load

on the bearing.

The computation technique involves first computing the load sharing between the balls in the absence of centrifugal forces. This involves a formalized trial and error (nesting type) procedure. Essentially, estimates of the axial and radial deflection of the bearing are made. The correct value of these deflections results in the correct radial and axial load.

REPRODUCIBILITY OF 1
ORIGINAL PAGE IS POOR

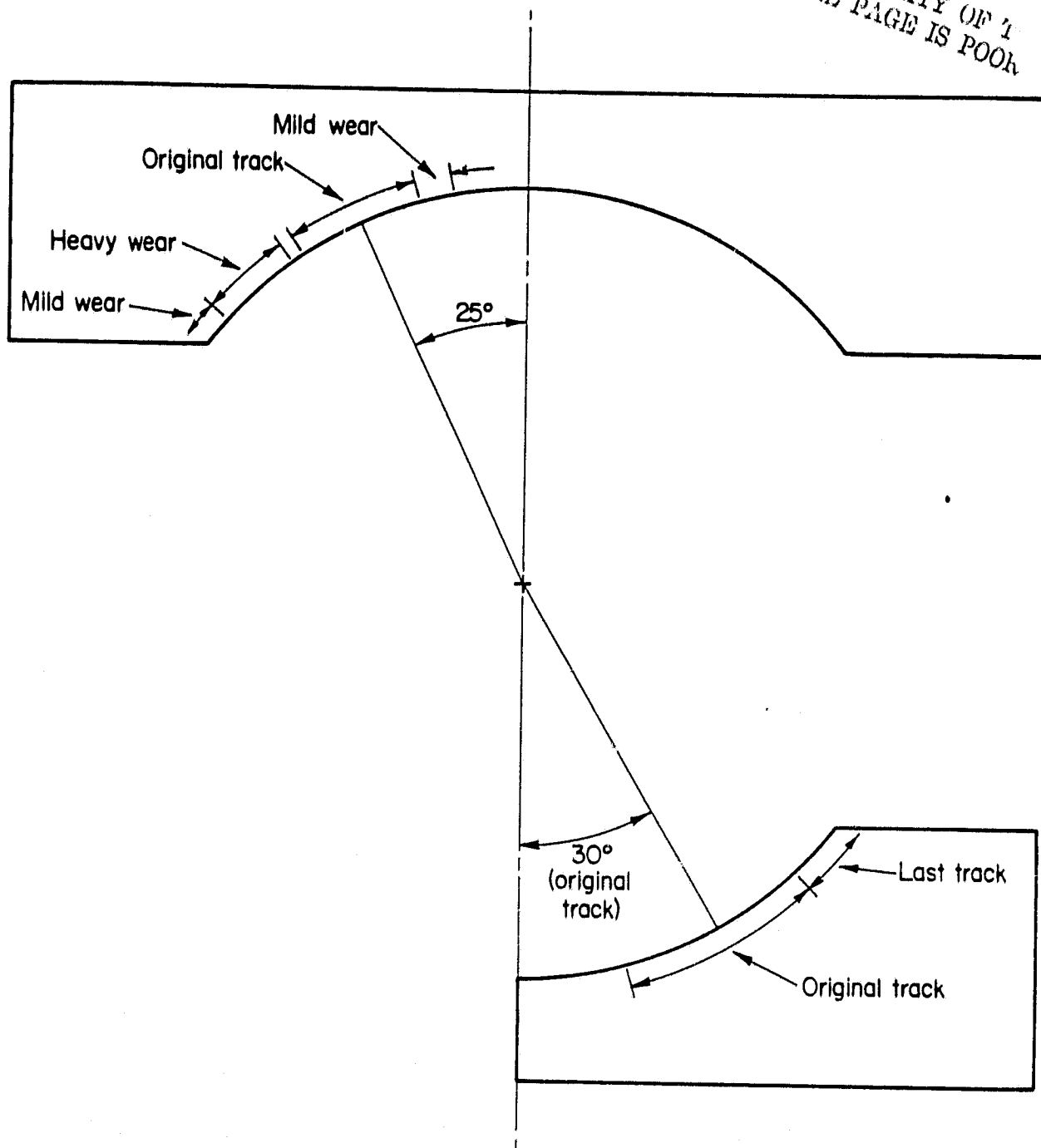


FIGURE 9. SUMMARY OF RACE EVALUATIONS

After the ball load sharing has been computed, the effect of centrifugal force on contact angle is computed. Essentially, this force causes the inner and outer race contact angles to be different from each other as well as different from the static contact angles. The method for the deflection and contact angles calculation is modeled after the classic work of A.B. Jones*.

Results of Calculations

The characteristics of the bearing that was analyzed are summarized in Table 1. The bearing is designed to operate at a static contact angle of 18.5 degrees. However, contact angle is a direct function of bearing diametral clearance and any wear of the balls or races will increase the effective contact angle. This increase in contact angle is accompanied by a drop in contact pressure as well as a drop in contact dimensions. Figures 10-12 show these changes in bearing dimensions as a function of diametral clearance increase for loads of 45 and 27 KN (10,000 and 6,000 pounds).

Although the bearing design load is in the 45-55 KN range, a load of 27 KN appears to fit initial wear scar measurements. For this load, the inner and outer contact angles are approximately 25 and 26 degrees and the contact width is 6 mm (0.24 inch) for the inner race and 5 mm (0.20 inch) for the outer race which is consistent with the measurements. If the diametral clearance is increased by 0.4 mm (0.016 inch) due to ball and race wear, the contact angles become 44 degrees for the inner race and 42 degrees for the outer race, and the outer and inner contact widths become 5 mm (0.20 inch) and 4.3 mm (0.17 inch), respectively. The effect of this .4 mm (.016 inch) clearance increase corresponds well with the final contact conditions observed for the bearing (see Figure 13). Note that the theoretical inner contact extends beyond the edge of the race, as was observed.

* Jones, A.B., "A General Theory for Elastically Constrained Ball and Roller Bearings Under Auxiliary Load and Speed Conditions", Trans. ASME, J. Basic Eng., Series D, Vol. 82, No. 2, June 1960, pp 309-320.

TABLE 1. PARAMETERS USED IN BEARING ANALYSIS

Parameter	Units	Value Assumed
Design Contact Angle	degrees	18.5
Outer Race Curvature	---	.53
Inner Race Curvature	---	.52
Number of Balls	---	13.
Ball Diameter	mm (inches)	20.6375 (.8125)
Pitch Diameter	mm (inches)	117.475 (4.625)
Bearing Speed	rpm	5000
Bearing Load	KN (pounds)	45 (10,000), 27 (6000)

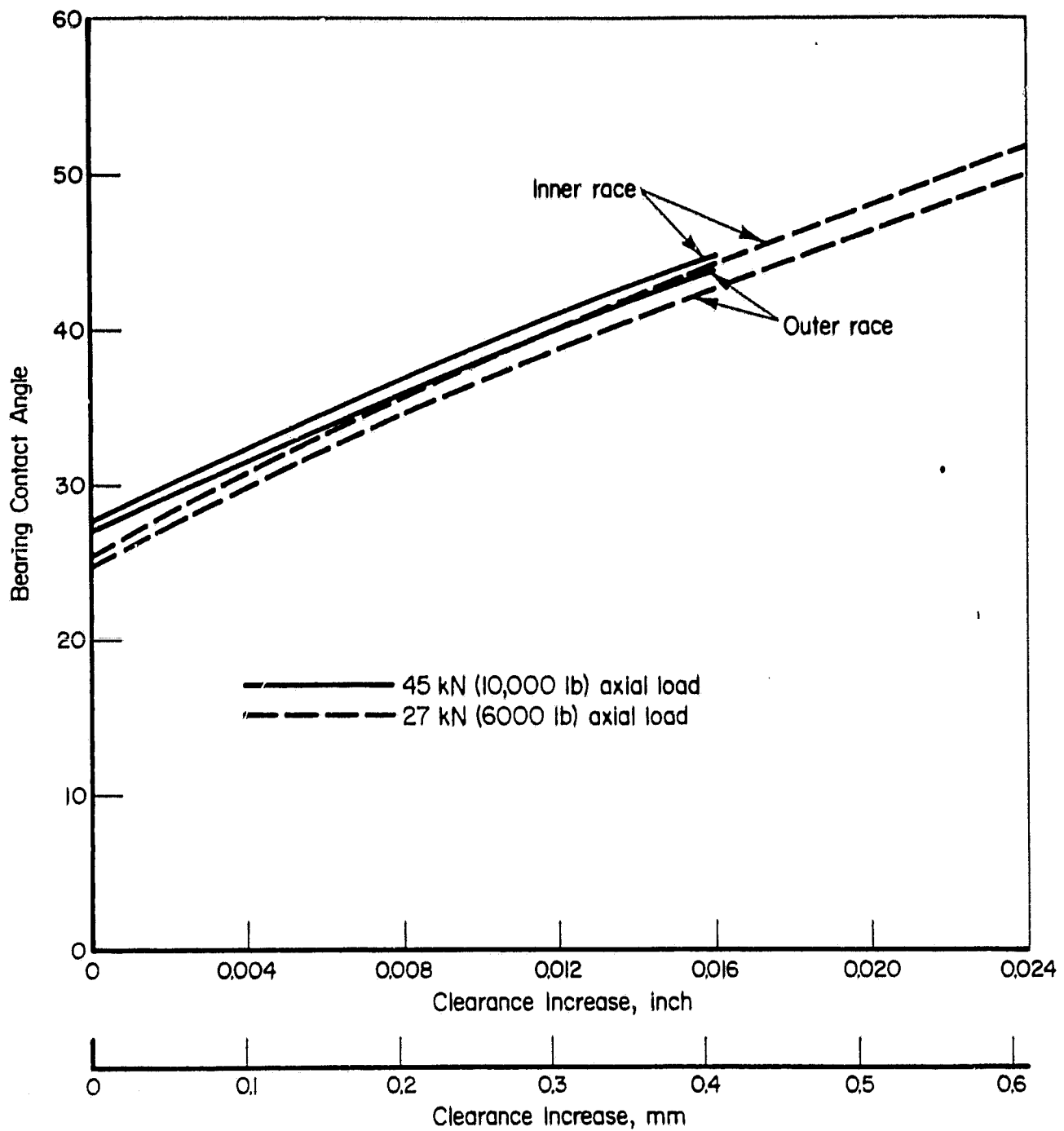


FIGURE 10. EFFECT OF DIAMETRAL CLEARANCE INCREASE ON BEARING CONTACT ANGLE

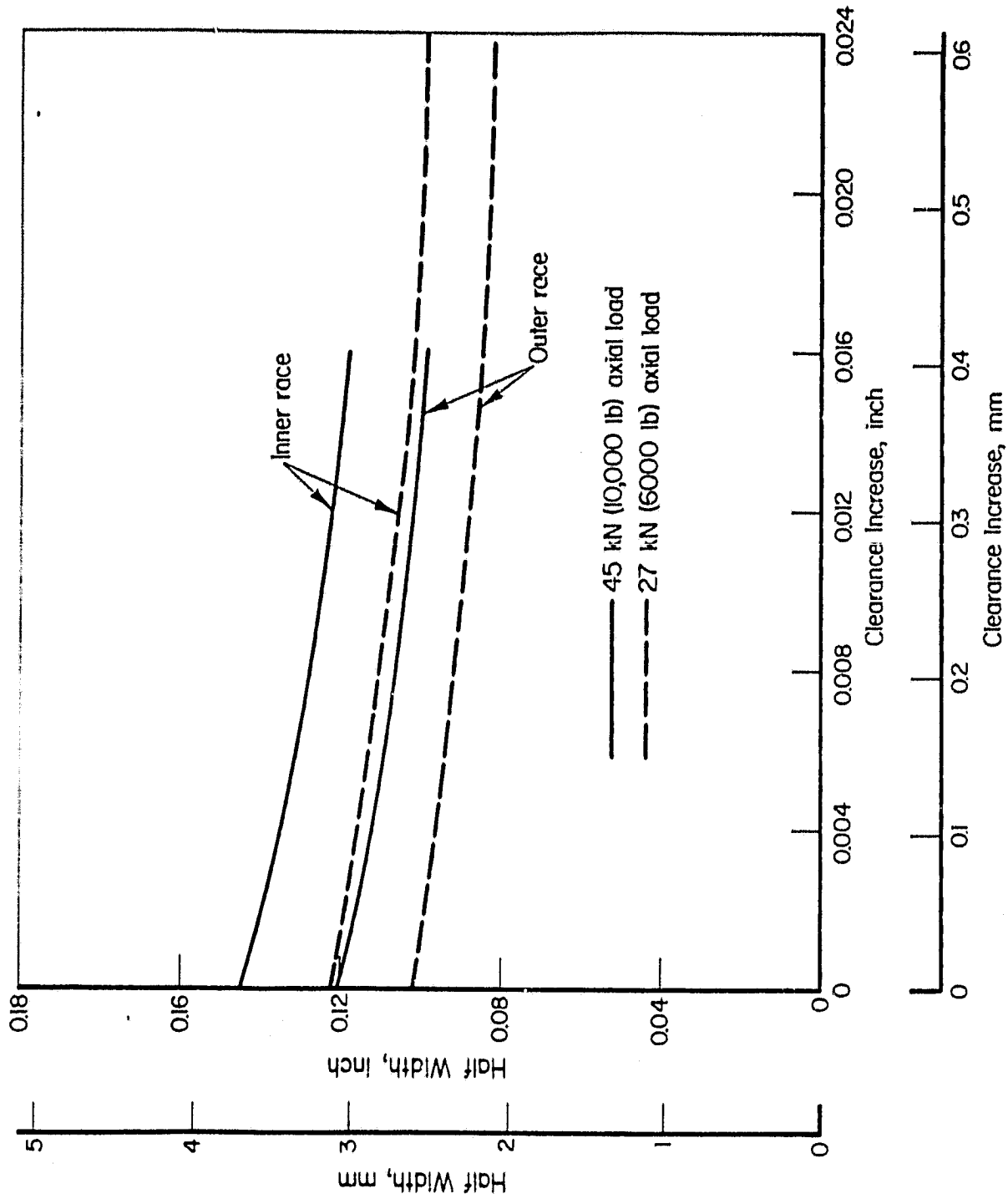


FIGURE 11. EFFECT OF DIAMETRAL CLEARANCE INCREASE ON HERTZ HALF WIDTH

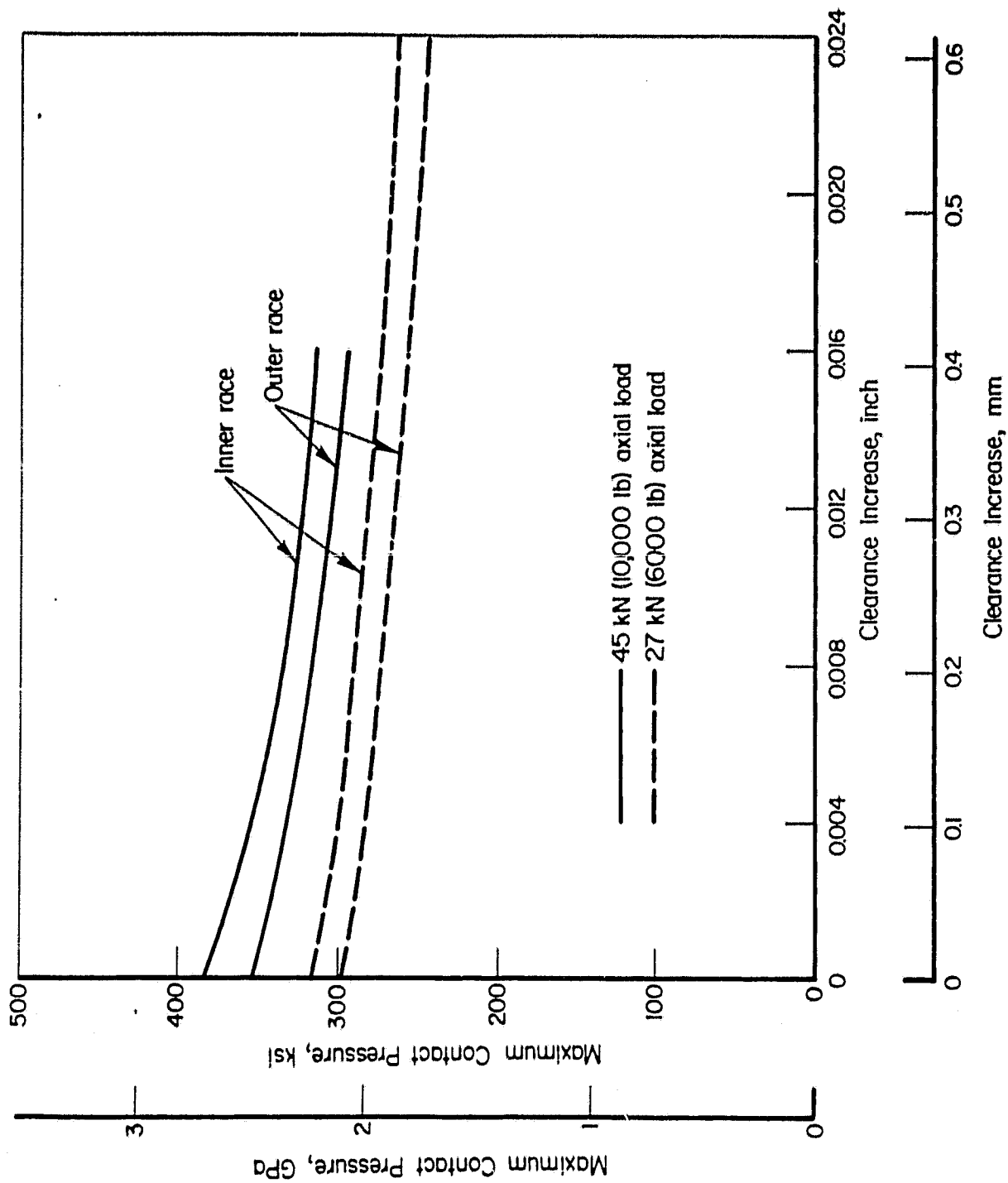


FIGURE 12. EFFECT OF DIAMETRAL CLEARANCE INCREASE ON CONTACT PRESSURE

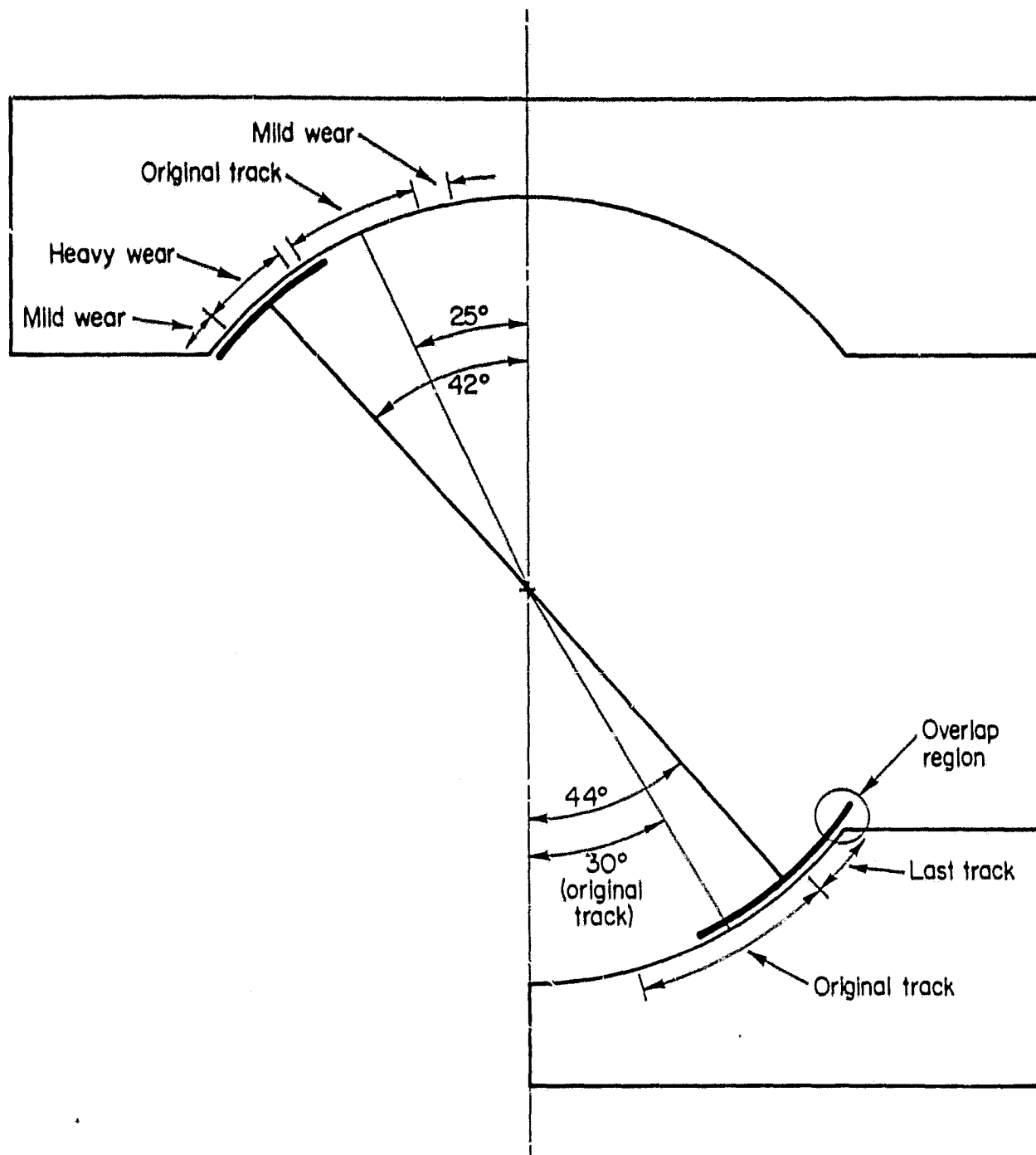


FIGURE 13. EFFECT OF .4 mm (.016 inch) DIAMETRAL CLEARANCE LOSS AND 6000 POUNDS AXIAL LOAD ON BEARING BALL-RACE CONTACT DIMENSIONS

On this basis, a reasonable scenario for the bearing distress is as follows:

- (1) The bearing was initially loaded to 6000 pounds axial load. The inner contact stress for this condition (see Figure 12) exceeded the allowable stress of 2.0 GPa (280,000 psi) for a transfer film lubricant and resulted in severe wear of the races and balls.
- (2) The combined wear on the balls and races eventually became as much as .4 mm (0.016 inch) and caused the inner ball-race contact to extend over the edge of the race.
- (3) With the ball "hanging-over" the race, the stresses were sufficient to plastically flow the races and further damage the balls.
- (4) Had the bearing not been removed from service, severe failure of the bearing probably would have occurred.

DISCUSSION

There are many possible reasons for a bearing to fail to perform its required function for an acceptable period of time. The two most common causes of failure are fatigue of the bearing steel and inadequate lubrication (accompanied by severe wear).

Fatigue Considerations

In 1947, Lundberg and Palmgren published a theory for the failure distribution of ball and roller bearings. This theory is summarized by

Coy, et al. in NASA TND-8362 (December 1976). Basically, the theory stated that bearing life can be expressed as

$$L_{10} = \left(\frac{K_1 z_0^h}{T_0^c V} \right)^{1/e} \quad (1)$$

where L_{10} = Life in millions of stress cycles

(based on 90 percent survival)

$K = 3.58 \times 10$ (based on 52100 steel, English units)

$e = 1.11$

$h = 2.334$

$c = 10.334$

V = stress volume ($z_0 l w$)

w = semi-width of rolling track

z_0 = depth of maximum shear stress

T_0 = maximum shear stress

l = length of rolling track.

Using the case postulated with 45 KN (10,000 pounds), axial load on bearing S/N-8383534:

$z_0 = .07$ inch

$T_0 = 114,000$ psi

$l = 12$ inches

$V = .12$ cubic inches

or

$L_{10} = 185$ million cycles or 95 hours of bearing operation.

The associated L_1 life (99 percent survival) is computed to be

$L_1 = 11$ hours.

This implies that bearing failure due to fatigue is not likely even with a higher axial load than is speculated to have occurred.

Lubrication Effects

Bearing performance depends heavily on the presence of some type of lubricant between the balls and races. There are two general types of lubricant films normally factored into bearing design: hydrodynamic and boundary. Hydrodynamic lubrication occurs as a result of the hydrodynamic action of the lubricant (normally a liquid) which forces a full film layer to form between ball and races. Under good hydrodynamic lubrication, a bearing will last indefinitely. Boundary lubrication occurs as a result of a chemical reaction between the lubricant, the lubricant additive, or dissolved oxygen in the lubricant with the metal surfaces. The "boundary films" are only a few monolayers thick and afford protection against cold welding of the surfaces. Both hydrodynamic and boundary films are necessary for good bearing performance. The hydrodynamic films keep the surfaces apart and the boundary films provide a back-up during start up or during partial full film loss due to high asperities, system dynamics, inadvertent high load or debris in the lubricant.

Since cryogenic fluids which are probably gaseous in ball-race contact regions are not considered to be suitable lubricants, the pump bearings must be lubricated by some other mechanism. This mechanism appears to be a pseudo-transfer film (retainer to ball) process. Such films have been observed in our examination of the bearing. The use of transfer films in high-speed, high-load applications is beyond the art of bearing technology and little is known of their assets or limitations. One limitation that is known is the allowable stress level. This level is on the order of 2 GPa (280,000 psi) maximum Hertz stress. Above this stress, the bearing elements are operating in metallic contact. A second limitation is the supply rate of the lubricant by the retainer wear process in the ball pockets. If this process is too high, the retainer wears out prematurely. If it is too low, inadequate lubrication results. Although significant retainer wear was measured, the wear rate may still be inadequate to supply the needed lubricant to the ball-race contacts.

Under poor lubrication conditions, considerable frictional forces between the balls and races will occur as a result of the ball spin on the non-controlling race. This friction force alters not only the surface shear stresses, but also the whole subsurface stress patterns. Under very high friction ($f \approx .2$) the maximum shear stress is on the surface.

Assuming Equation (1) is valid, it can be seen that

$$L_{10} \propto z_0^{1.2}, \quad (2)$$

where, as mentioned before, z_0 is the depth to the maximum shear stress. Obviously, as the maximum stress approaches the surface, bearing life approaches "zero".

The above calculations indicate that in order to optimize bearing performance, it is mandatory that, as a minimum, adequate transfer film lubrication must be maintained. This means that the stresses in the bearing must be kept below 2 GPa (280,000 psi). With the current configuration, achieving this stress level is very difficult as shown in Figure 12. It is thus recommended that a redesign of the bearing be undertaken.

Measuring Units

Since the bearing drawings and all input data provided by NASA were in English units, all measurements and calculations were performed in English units. Therefore, the SI units presented in this report were converted from English units. Data on which this report is based are located in Battelle Laboratory Record Book No. 34405.